Gravity perturbed Crapper waves

Benjamin F. Akers, David M. Ambrose and J. Douglas Wright

References	**This article cites 45 articles, 1 of which can be accessed free** http://rspa.royalsocietypublishing.org/content/470/2161/2013052 6.full.html#ref-list-1
Subject collections	Articles on similar topics can be found in the following collections applied mathematics (311 articles)
Email alerting service	Receive free email alerts when new articles cite this article - sign up in the box at the top right-hand corner of the article or click **here**

Author for correspondence:
David M. Ambrose
e-mail: ambrose@math.drexel.edu

Gravity perturbed Crapper waves

Benjamin F. Akers[1], David M. Ambrose[2] and J. Douglas Wright[2]

[1]Department of Mathematics and Statistics, Air Force Institute of Technology, Dayton, OH, USA
[2]Department of Mathematics, Drexel University, 3141 Chestnut Street, Philadelphia, PA, USA

Crapper waves are a family of exact periodic travelling wave solutions of the free-surface irrotational incompressible Euler equations; these are pure capillary waves, meaning that surface tension is accounted for, but gravity is neglected. For certain parameter values, Crapper waves are known to have multi-valued height. Using the implicit function theorem, we prove that any of the Crapper waves can be perturbed by the effect of gravity, yielding the existence of gravity–capillary waves nearby to the Crapper waves. This result implies the existence of travelling gravity–capillary waves with multi-valued height. The solutions we prove to exist include waves with both positive and negative values of the gravity coefficient. We also compute these gravity perturbed Crapper waves by means of a quasi-Newton iterative scheme (again, using both positive and negative values of the gravity coefficient). A phase diagram is generated, which depicts the existence of single-valued and multi-valued travelling waves in the gravity–amplitude plane. A new largest water wave is computed, which is composed of a string of bubbles at the interface.

1. Introduction

We study the irrotational, incompressible Euler equations for a fluid bounded above by a free surface, with vacuum above the free surface. We consider a fluid region that is infinitely deep in the vertical direction and periodic in the horizontal direction. We seek travelling wave solutions, or solutions for which the free surface is of permanent form and steadily translating. We consider the effect of surface tension at the fluid boundary.

For this problem, in the absence of gravity, a family of exact solutions is known; these solutions are called Crapper waves, as they were discovered by Crapper [1]. There is an exposition of these waves in the book of Crapper [2], and also, in more detail, in the book of Kinsman [3]. A formula for Crapper waves is given in §2.

Kinnersley extended the Crapper waves to the case of finite depth [4]. As in the infinite depth case that Crapper studied [1], the travelling waves are found as exact solutions, in this case involving elliptic functions. Building upon the work by Tanveer for translating bubbles [5], Crowdy gives a different derivation of the Crapper waves, using conformal maps [6]. The formulation of Crowdy also allows for the identification of other, previously unknown, exact solutions of the free-surface Euler equations with surface tension. Crowdy further shows that exact steady free-surface Euler flows such as the Crapper waves yield, through a transformation, exact steady Hele–Shaw flows [7].

Uniqueness and stability of Crapper waves have also been studied. Assuming a certain positivity condition, Okamoto has proved uniqueness of the Crapper waves (that is, any travelling pure capillary water wave on infinite depth that satisfies the positivity condition is a Crapper wave) [8]; see also the discussion in the book of Okamoto & Shōji [9]. Tiron & Choi [10] studied stability of the Crapper waves. Stability was also studied by Hogan [11] and by Chen & Saffman [12].

Given an exact solution or family of exact solutions of a nonlinear partial differential equation, a natural question to ask is, can we perturb these solutions to find other, nearby solutions? Since the Crapper waves are irrotational, pure capillary water waves, there are then several natural directions in which to perturb them: through the inclusion of gravity, through the inclusion of vorticity in the bulk of the fluid and through the addition of an upper fluid to replace the vacuum above the waves. In this contribution, we prove that it is indeed possible to perturb any Crapper wave solution through the inclusion of gravity, either positive or negative. We do this by using a modified Liapunov–Schmidt analysis. We call the waves we find gravity perturbed Crapper waves. Perturbing the Crapper waves with vorticity or an additional fluid is expected to be the subject of future research.

In addition to proving they exist, we compute gravity perturbed Crapper waves and study the differences in features of the waves caused by the presence of gravity. The computational method used is the method introduced by the authors in [13]. This method uses a normalized arclength parametrization of the free surface, as developed for a numerical method for initial-value problems for vortex sheets in [14,15] and used analytically (again for the initial-value problem) in [16]. Since we describe waves using the arclength parametrization, there is no assumption that the interface has single-valued height, and thus the method works in exactly the same way whether or not the interface has overturned.

A number of other papers have computed overturning travelling waves in free-surface Euler flows. Baker *et al.* [17] formulated the travelling wave problem in such a way as to allow for overturning waves, but only computed waves with single-valued height in interfacial flows. Other studies that computed interfacial waves with multi-valued height are those of Saffman & Yuen [18], Meiron & Saffman [19], Turner & Vanden-Broeck [20] and Grimshaw & Pullin [21].

The self-intersection and extreme forms of gravity–capillary waves have been studied previously. In particular, a detailed study was made by Hogan [22]. The method of Hogan [22] is a boundary perturbation method, in the style of the expansions of Stokes [23] and Wilton [24,25]. Similar boundary perturbation methods have been applied to the water wave problem, with and without surface tension [26–31]. As noted in [30], these methods can be susceptible to floating point instabilities. Hogan observed this problem in his results, and reacted by working in quadruple precision and restricting the number of terms in his series expansions. The transformed field expansions method (of Nicholls and collaborators), a boundary perturbation algorithm, is stable to such errors [30,31]; however, it cannot compute overturned travelling waves.

A popular alternative to boundary perturbation is the combination of Fourier collocation and a quasi-Newton solver. Such an approach has been applied to compute gravity–capillary waves in a variety of settings, including finite and infinite depth, periodic and solitary waves [32]. For

overturning waves, the majority of these computations are based on a conformal mapping applied to the fluid domain. The closest works in this latter class to the present are those of Debiane & Kharif [33] and Debiane *et al.* [34], in which the largest travelling waves are computed for a sampling of Bond numbers, that of Schwartz & Vanden-Broeck [35], where a host of travelling waves are computed at various amplitudes and Bond numbers, and Vanden-Broeck & Keller [36] computed the analogue of Crapper waves with larger bubbles (by varying the internal bubble pressure). Our numerical method also uses Fourier collocation and a quasi-Newton solver, but rather than being based on a conformal mapping, it instead parametrizes the interface by arclength [13]. This allows us to keep a uniform grid spacing along the interface, as opposed to having our grid points chosen by the mapping.

To complement our existence results, we numerically compute wave profiles and speeds, varying both the amplitude and the Bond number $\sigma = g/k^2\tau$ (these quantities will be specified in more detail in the sequel). The Bond number is the relevant non-dimensional quantity measuring the relative importance of gravity and surface tension. It is common to see the inverse of this quantity also called the Bond number; we choose this version of the Bond number as it is bounded near the Crapper wave at $g = 0$. Because the existence proof relies on the implicit function theorem, it does not require that gravity be positive; therefore, in our computations, we perturb the Crapper wave with both positive and negative Bond number. We compute continuous branches of travelling waves connecting Crapper waves ($\sigma = 0$) to gravity–capillary waves with $\sigma = 20$, as well as to waves with negative Bond number $-1 < \sigma < 0$. Unlike methods based on amplitude expansions, our method need not be altered to compute the resonant Wilton ripples [37,38]. Our results support the conclusions of Schwartz & Vanden-Broeck [35]; we observe travelling waves at the Wilton ripple Bond numbers that are continuously embedded among the travelling waves computed elsewhere.

For the branches of waves bifurcating from the Crapper waves that we compute, as Bond number increases, we observe that the Crapper wave is continuously connected to *solitary* gravity–capillary waves. These computations serve as numerical verification of the argument of Longuet–Higgins, whereby asymptotics about the Crapper wave are used to approximate gravity–capillary solitary waves [39]. For the branches of waves with $\sigma < 0$, we observe that the large-amplitude limit is typically a stationary (or standing) wave, rather than a travelling wave with a self-intersecting profile. We have generated a phase portrait of the existence of multi-valued and single-valued travelling waves in the gravity–amplitude plane. A new, globally largest water wave is computed, which is both standing and self-intersecting. This wave consists of a string of bubbles and droplets at the fluid interface.

The paper is organized as follows: in §2, we describe Crapper waves. In §3, we give our proof, using the implicit function theorem, to show the existence of gravity perturbed Crapper waves. In §4, we describe our numerical method and give our numerical results.

2. Crapper waves

In §1.1 of the book of Okamoto & Shōji [9], they give the following equation whose solutions give travelling spatially periodic gravity–capillary waves in a two-dimensional fluid of infinite depth:

$$F(\theta; p, q) := e^{2H\theta} \frac{dH\theta}{da} - p\, e^{-H\theta} \sin(\theta) + q\frac{d}{da}\left(e^{H\theta}\frac{d\theta}{da}\right) = 0. \tag{2.1}$$

Here, the independent variable a is in $\mathbf{T} := [-\pi, \pi]$, θ is the tangent angle to the surface and satisfies periodic boundary conditions, and H is the periodic Hilbert transform,

$$Hf(a) := \frac{1}{2\pi} \mathrm{PV} \int_{-\pi}^{\pi} \cot\left(\frac{1}{2}(a - s)\right) f(s)\, ds.$$

For background on the periodic Hilbert transform, the interested reader could consult, for instance, [40]. The non-dimensional constants p and q are given by

$$p := \frac{gL}{2\pi c^2} \quad \text{and} \quad q := \frac{2\pi\tau}{\rho c^2 L},$$

where L is the spatial period of the wave, c is the travelling wave speed, g is the acceleration due to gravity and τ is the surface tension constant. We remark that in the sequel, we will always take q to be positive. This formulation of the travelling water wave problem follows from complex variable methods initiated by Stokes [23], with important contributions from Levi-Civita [41].

An important feature here is that the free surface is not parametrized by arclength; reconstruction of the surface from θ requires some more information. Specifically, if $\theta(a)$ is a solution of (2.1), the parametrization of the free surface $(x(a), y(a))$ is given by

$$\left. \begin{aligned} \frac{dx}{da} &:= -\frac{L}{2\pi} \, e^{-H\theta(a)} \cos(\theta(a)) \\ \frac{dy}{da} &:= -\frac{L}{2\pi} \, e^{-H\theta(a)} \sin(\theta(a)). \end{aligned} \right\} \tag{2.2}$$

and

If one sets $p = 0$, then one can find exact formulae for solutions θ of (2.1), which are called *Crapper waves*. We briefly explain these solutions now. When $p = 0$, (2.1) becomes

$$e^{2H\theta} \frac{dH\theta}{da} + q \frac{d}{da}\left(e^{H\theta} \frac{d\theta}{da}\right) = 0.$$

The left-hand side is a perfect derivative,

$$\frac{d}{da}\left(\frac{1}{2} e^{2H\theta} + q \, e^{H\theta} \frac{d\theta}{da}\right) = 0.$$

Integrating gives

$$\frac{1}{2} e^{2H\theta} + q \, e^{H\theta} \frac{d\theta}{da} = \text{const.} \tag{2.3}$$

In [9], the following is shown.

Lemma 2.1. *For any $\theta \in L^2(\mathbf{T})$,*

$$\int_{-\pi}^{\pi} e^{\pm H\theta(a) - i\theta(a)} \, da = 2\pi. \tag{2.4}$$

With this, one can show that the constant in (2.3) is $1/2$. Equation (2.3) can then be rewritten as

$$q\frac{d\theta}{da} + \sinh(H\theta) = 0. \tag{2.5}$$

Take $q \geq 1$ and let A be either of the solutions of

$$q = \frac{1 + A^2}{1 - A^2}.$$

Note that $A \in (-1, 1)$. Let

$$\omega(z) := 2i \log\left(\frac{1 + Az}{1 - Az}\right)$$

and

$$\theta_q(a) := \Re\omega(e^{ia}).$$

Then, we have the following.

Theorem 2.2 (Crapper [1]).

$$q\frac{d\theta_q}{da} + \sinh(H\theta_q) = 0.$$

Note that $\theta_q(a)$ is an odd function of a. The function θ_q gives the Crapper wave.

Linearizing (2.5) about θ_q gives the operator

$$\Gamma u := q u' + \cosh(H\theta_q) H u.$$

(Here and below, the prime indicates differentiation with respect to a.) The following lemma, which is equivalent to [9, lemma 2.1], is used there to prove that the Crapper waves are locally unique.

Lemma 2.3 (Okamoto & Shōji [9]). *For $q > 1$, zero is an eigenvalue of $\Gamma : X^1 \to L^2(\mathbf{T})$ with geometric multiplicity one and algebraic multiplicity two. The eigenfunction is $\mathrm{d}\theta_q/\mathrm{d}a$ and the generalized eigenfunction is $\partial\theta_q/\partial q$.*

In the above,

$$X^s := \{f \in H^s(\mathbf{T}) : (f, 1) = 0\}$$

and

$$(f, v) := \int_{-\pi}^{\pi} f(a)v(a)\,\mathrm{d}a.$$

In this article, we show that Crapper waves perturb to solutions of (2.1) when $p \sim 0$. In particular, we prove the following theorem.

Theorem 2.4. *For all $q > 1$, there exist $P = P(q) > 0$ and a C^∞ function*

$$\Theta_q : (-P, P) \longrightarrow X^2$$

such that $F(\Theta_q(p); p, q) = 0$ for $|p| < P$ and $\Theta_q(0) = \theta_q$. Moreover, $\Theta_q(p)$ is an odd function of a, and Θ_q is smooth with respect to q.

Remark 2.5. Note that this theorem gives the existence of travelling gravity–capillary waves nearby to the Crapper waves, for small values of p, with either $p > 0$ or $p < 0$, i.e. with either positive or negative values of the acceleration due to gravity. There are some theorems in the literature on the non-existence of travelling water waves with negative gravity, in the case of pure gravity waves [42,43].

The method of proof is, roughly speaking, a Liapunov–Schmidt analysis, and follows relatively quickly from theorem 2.2 and lemma 2.3. Despite the brevity of its proof, we point out a particularly important and novel feature of theorem 2.4: it implies the existence of periodic travelling capillary–gravity waves that overhang. It is well known that for q large enough, the profile of the Crapper wave is not given by a function over the horizontal Eulerian coordinate. As our theorem applies for any $q > 1$ and Θ_q is continuous with respect to p, we have the same feature for the gravity perturbed Crapper wave.

We will be employing the implicit function theorem several times in our proof and for completeness, we state the version of this theorem we use here.

Theorem 2.6 (The implicit function theorem). *X, Y and Z are Banach spaces and $\zeta : X \times Y \to Z$ is C^k, $k \geq 1$. If $\zeta(x^*, y^*) = 0$ and $D_x\zeta(x^*, y^*)$ is a bijection from X to Z, then there exists $\epsilon > 0$ and a unique C^k map $\chi : Y \to X$ such that $\chi(y^*) = x^*$ and $\zeta(\chi(y), y) = 0$ when $\|y - y^*\|_Y < \epsilon$.*

Statements of implicit function theorems can be found in many standard texts; for example, a similar statement to theorem 2.6 can be found in [44, ch. 13].

3. Existence of gravity perturbed Crapper waves

Our first task is to rewrite the problem (2.1) as a perturbation of (2.5). Note that we can write (2.5) as

$$\frac{d}{da}\left[\frac{1}{2}e^{2H\theta} + q e^{H\theta}\theta'\right] - p e^{-H\theta}\sin(\theta) = 0.$$

Integrating this from 0 to a, we get

$$\frac{1}{2}e^{2H\theta} + q e^{H\theta}\theta' - p\int_0^a e^{-H\theta(a')}\sin(\theta(a'))\,da' = \gamma, \tag{3.1}$$

where γ is a constant. Note that it is possible to determine the value of γ in advance for a solution, as is done in the derivation of (2.5) above. However, it is to our advantage in the proof to leave this constant undetermined at this time, as it gives us an extra parameter at our disposal. Recalling the constant of integration when $p = 0$ was $1/2$, we set

$$\gamma = \frac{1}{2} + \kappa,$$

where $\kappa \in \mathbf{R}$. Also, we define

$$I(\theta)(a) := \int_0^a e^{-H\theta(a')}\sin(\theta(a'))\,da'.$$

We then recast (3.1) as

$$\frac{1}{2}e^{2H\theta} + q e^{H\theta}\theta' - pI(\theta) - \frac{1}{2} - \kappa = 0.$$

A quick rearrangement of terms converts this to

$$\Phi(\theta; p, \kappa) := q\theta' + \sinh(H\theta) - p e^{-H\theta}I(\theta) - \kappa e^{-H\theta} = 0. \tag{3.2}$$

Observe that theorem 2.2 shows that $\Phi(\theta_q; 0, 0) = 0$. Moreover, if we linearize Φ at $\theta = \theta_q$ and $p = \kappa = 0$, we have

$$D_\theta \Phi(\theta_q; 0, 0) = \Gamma.$$

Lemma 2.3 tells us that Γ is not invertible. As such, we cannot directly employ the implicit function theorem to find solutions of $\Phi = 0$.

Nevertheless, we can eliminate the kernel of Γ by restricting attention to odd functions. Let

$$X_{\mathrm{odd}}^1 := \{f \in H^1(\mathbf{T}) : f \text{ is odd}\}$$

and

$$Y_{\mathrm{even}}^0 := \{f \in L^2(\mathbf{T}) : f \text{ is even}\}.$$

Of course X_{odd}^1 is a subspace of X^1 and Y_{even}^0 is a subspace of $L^2(\mathbf{T})$.

Proposition 3.1. $\Phi(\theta; p, \kappa)$ is a C^∞ map from $X_{\mathrm{odd}}^1 \times \mathbf{R}^2$ into Y_{even}^0.

We omit the proof of this. The key thing is that d/da, H and I all map odd functions to even ones.

Recall that θ_q is odd, and thus θ_q' is even. Therefore, the kernel of Γ as a map on X_{odd}^1 is trivial. That is, we have the following corollary of lemma 2.3.

Corollary 3.2. When Γ is viewed as a map from X_{odd}^1 to Y_{even}^0,

$$\ker \Gamma = \{0\}.$$

It might at this time appear that we could apply the implicit function theorem to find solutions of (3.2). However, this is not the case. While Γ is injective as a map from X_{odd}^1 to Y_{even}^0, it is not surjective, as the following proposition demonstrates.

Proposition 3.3. *Let* $f \in Y^0_{\text{even}}$. *Then, there exists* $u \in X^1_{\text{odd}}$ *with*

$$\Gamma u = f$$

if and only if

$$(f, \cos(\theta_q)) = 0.$$

Proof. Lemma 2.1 implies, for any function $w \in L^2(\mathbf{T})$,

$$\int_{-\pi}^{\pi} e^{-iw(a)} \sinh(Hw(a)) \, da = 0.$$

Taking the real part of this gives

$$\int_{-\pi}^{\pi} \cos(w(a)) \sinh(Hw(a)) \, da = 0.$$

Also, as $d/da \sin(w(a)) = \cos(w(a)) w'(a)$, we have $\int_{-\pi}^{\pi} \cos(w(a)) w'(a) \, da = 0$. So, for any function $w \in H^1(\mathbf{T})$,

$$\int_{-\pi}^{\pi} \cos(w(a))[\sinh(Hw(a)) + qw'(a)] \, da = 0. \tag{3.3}$$

Fix $u \in H^1(\mathbf{T})$ and let $w = \theta_q + \epsilon u$, where $\epsilon \in \mathbf{R}$. Inserting this into (3.3) gives, for all ϵ,

$$\int_{-\pi}^{\pi} \cos(\theta_q(a) + \epsilon u(a))[\sinh(H\theta_q(a) + \epsilon Hu(a)) + q\theta_q'(a) + \epsilon qu'(a)] \, da = 0.$$

Differentiating this with respect to ϵ, and then setting $\epsilon = 0$ gives

$$- \int_{-\pi}^{\pi} \sin(\theta_q(a)) u(a)[\sinh(H\theta_q(a)) + q\theta_q'(a)] \, da$$

$$+ \int_{-\pi}^{\pi} \cos(\theta_q(a))[\cosh(H\theta_q(a)) Hu(a) + qu'(a)] \, da = 0.$$

The first line vanishes by theorem 2.2. The term in square brackets in the second line is Γu. Thus, we have, for all $u \in H^1(\mathbf{T})$,

$$\int_{-\pi}^{\pi} \cos(\theta_q(a)) \Gamma u(a) \, da = (\Gamma u, \cos(\theta_q)) = 0. \tag{3.4}$$

If $f \in Y^0_{\text{even}}$ and $u \in X^1_{\text{odd}}$ satisfy $\Gamma u = f$, then (3.4) tells us

$$(f, \cos(\theta_q)) = 0.$$

And so we have shown the 'only if' part of the proposition.

To finish the proof, we need to show that if $f \in Y^0_{\text{even}}$ and $(f, \cos(\theta_q)) = 0$, then there exists $u \in X^1_{\text{odd}}$ with $\Gamma u = f$. First, note that

$$Ku := \cosh(H\theta_q) Hu$$

defines a bounded map from X^1_{odd} to Y^0_{even}. It is also bounded from $L^2(\mathbf{T})$ to itself. Suppose that $\{u_n\} \subset X^1_{\text{odd}}$ is a bounded sequence. As $X^1_{\text{odd}} \subset H^1(\mathbf{T}) \subset\subset L^2(\mathbf{T})$ (owing to the Rellich–Kondrachov theorem), we know $\{u_n\}$ contains a subsequence that converges in $L^2(\mathbf{T})$. We abuse notation and call this subsequence $\{u_n\}$. Since the functions u_n are odd, so is the limit. Also, K is bounded on $L^2(\mathbf{T})$, and thus $\{Ku_n\}$ is a convergent sequence of even functions in $L^2(\mathbf{T})$. The limit is even. Thus, K is a compact operator from X^1_{odd} to Y^0_{even}.

Now, $\Gamma u = qu' + K$, which means that Γ is a compact perturbation of

$$\Gamma_0 := q\frac{d}{da}.$$

We claim that Γ_0 is a Fredholm operator from X^1_{odd} to Y^0_{even} with index -1. This is straightforward. We recall that q is non-zero and that the kernel of d/da is the set of constant functions. The only odd constant function is 0. Therefore, the kernel of Γ_0 in X^1_{odd} is trivial. Likewise, $\Gamma_0 u = f$ has

a periodic solution u if and only if $\int_{-\pi}^{\pi} f(a') \, da' = 0$. This implies that the cokernel of Γ_0 is one dimension. Thus, the index of Γ_0 is -1.

As compact perturbations do not change the index of an operator [44], we know that Γ is also a Fredholm operator from X_{odd}^1 to Y_{even}^0 with index -1. As we know the kernel of Γ is trivial from corollary 3.2, we must therefore have that the dimension of the cokernel of Γ is equal to 1.

As $(\cos(\theta_q), \cos(\theta_q)) \neq 0$, the work above tells us that $\cos(\theta_q)$ is not in the range of Γ. Thus, the equivalence class of this function, which we call $[c]$, spans the cokernel of Γ. Now take $f \in Y_{\mathrm{even}}^0$ with $(f, \cos(\theta_q)) = 0$. Let $[f]$ be the equivalence class of f in the cokernel. There must be a constant $\beta \in \mathbf{R}$ such that $[f] = \beta[c]$. This means that there exists $u \in X_{\mathrm{odd}}^1$ with $\Gamma u = f - \beta \cos(\theta_q)$. From the first part of this proof, we know that this implies $(f - \beta \cos(\theta_q), \cos(\theta_q)) = 0$, which implies $\beta = 0$. This in turn implies that $\Gamma u = f$, and we are done. ∎

So Γ is not surjective. Our method is a modification of the Liapunov–Schmidt strategy commonly used in perturbation theory when the linearization of the problem fails to be injective to the case when the problem fails to be surjective. Define

$$\Pi u := \mu (\cos(\theta_q), u) \cos(\theta_q),$$

where $\mu := (\cos(\theta_q), \cos(\theta_q))^{-1}$. A quick calculation shows $\Pi^2 = \Pi$, and so Π is a projection. Moreover, (3.4) tells us that

$$\Pi \Gamma = 0. \tag{3.5}$$

Let $R := \ker \Pi$ and $M := R^{\perp}$. Proposition 3.3 tells us that $R = \Gamma(X_{\mathrm{odd}}^1)$. Let

$$\Phi_{\mathrm{red}}(\theta; p, \kappa) = (1 - \Pi)\Phi(\theta; p, \kappa).$$

Note that $\Pi \Phi_{\mathrm{red}} = (\Pi - \Pi^2)\Phi = 0$, and so Φ_{red} is a map from $X_{\mathrm{odd}}^1 \times \mathbf{R}^2$ into R.

From theorem 2.2, we know

$$\Phi_{\mathrm{red}}(\theta_q; 0, 0) = 0.$$

Also,

$$D_\theta \Phi_{\mathrm{red}}(\theta_q; 0, 0) = (1 - \Pi)\Gamma.$$

As $\Pi \Gamma = 0$, we see that $(1 - \Pi)\Gamma$ is injective because Γ is. Moreover, by construction, $(1 - \Pi)\Gamma$ is surjective onto R. And thus we can, at last, apply the implicit function theorem: there exists a unique C^∞ map

$$\Xi(p, \kappa) : \mathbf{R}^2 \to X_{\mathrm{odd}}^1,$$

so that

$$\Phi_{\mathrm{red}}(\Xi(p, \kappa); p, \kappa) = (1 - \Pi)\Phi(\Xi(p, \kappa); p, \kappa) = 0,$$

for all (p, κ) sufficiently small and

$$\Xi(0, 0) = \theta_q.$$

Now set

$$g(p, \kappa) := \frac{\Pi \Phi(\Xi(p, \kappa); p, \kappa)}{\mu \cos(\theta_q)} = (\cos(\theta_q), \Phi(\Xi(p, \kappa); p, \kappa)).$$

This is a map from $\mathbf{R}^2$ to itself. That is to say, $g(p, \kappa)$ satisfies $\Pi \Phi(\Xi(p, \kappa); p, \kappa) = \mu g(p, \kappa) \cos(\theta_q)$. If we find $g(p^*, \kappa^*) = 0$, then note that $\Xi(p^*, \kappa^*)$ has

$$\Phi(\Xi(p^*, \kappa^*); p^*, \kappa^*) = \Pi \Phi(\Xi(p^*, \kappa^*); p^*, \kappa^*) + (1 - \Pi)\Phi(\Xi(p^*, \kappa^*); p^*, \kappa^*) = 0.$$

That is to say, it solves (3.2).

Clearly, $g(0,0) = 0$. We claim that

$$D_\kappa g(0,0) = -2\pi. \tag{3.6}$$

If so, we can call again on the implicit function theorem. This tells us that there exists a unique map, $\xi(p)$, smooth, with $\xi(0) = 0$ and defined for p sufficiently small, for which

$$g(p, \xi(p)) = 0.$$

(Note that this function $\xi(p)$ selects κ and thus γ.) Let

$$\Theta_q(p) := \Xi(p, \xi(p)).$$

This is the map whose existence we were hoping to establish. There are two things left to check. The first is to establish (3.6) and the second is to show that $\Theta_q(p) \in X^2$, not just X^1_{odd}. This latter is important in that a solution of (3.2) in X^2 will also be a solution of (2.1), which is our ultimate goal. We mention that the smoothness of Θ_q with respect to q follows from our repeated use of the implicit function theorem.

For (3.6), note that

$$D_\kappa g(0,0) = \frac{\Pi[\Gamma \Xi_\kappa(0,0) + D_\kappa \Phi(\theta_q;0,0)]}{\mu \cos(\theta_q)}.$$

As $\Pi\Gamma = 0$, we have

$$D_\kappa g(0,0) = \frac{\Pi D_\kappa \Phi(\theta_q;0,0)}{\mu \cos(\theta_q)}.$$

Then, we see from (3.2) that $D_\kappa \Phi(\theta_q;0,0) = -e^{-H\theta_q}$, and therefore

$$D_\kappa g(0,0) = -\frac{\Pi e^{-H\theta_q}}{\mu \cos(\theta_q)} = -(e^{-H\theta_q}, \cos(\theta_q)) = -\int_{-\pi}^{\pi} e^{-H\theta_q(a)} \cos(\theta_q(a)) \, da$$

$$= -\frac{1}{2}\int_{-\pi}^{\pi} e^{-H\theta_q(a)+i\theta_q(a)} \, da - \frac{1}{2}\int_{-\pi}^{\pi} e^{-H\theta_q(a)-i\theta_q(a)} \, da.$$

Using lemma 2.1, we have $D_\kappa g(0,0) = -2\pi$, as claimed.

Finally, let $\theta := \Theta_q(p)$. We know that $\theta \in X^1_{odd} \subset H^1(\mathbf{T})$ and that θ solves (3.2). Since $\theta \in H^1(\mathbf{T})$, we know $H\theta \in H^1(\mathbf{T})$ as well. This in turn implies that $\sinh(H\theta)$ and $e^{-H\theta}$ are in $H^1(\mathbf{T})$. Likewise for $I(\theta)$. Thus,

$$\rho := \sinh(H\theta) - p\,e^{-H\theta} I(\theta) - \kappa\,e^{-H\theta} \in H^1(\mathbf{T}).$$

It is straightforward to see that as θ depends smoothly on p, so must ρ. As (3.2) states that $\theta' = -(1/q)\rho$, we have $\theta' \in H^1(\mathbf{T})$, and thus $\theta \in H^2(\mathbf{T})$. Therefore, we can differentiate (3.2) to see that θ solves (2.1) and depends smoothly on p. (We remark that this argument could be repeated to conclude higher regularity of θ.) This completes the proof of theorem 2.4.

4. Numerical results

In this section, we augment the preceding existence proof with numerical computations of branches of travelling waves bifurcating from the Crapper waves. The branches are computed in the arclength parametrized vortex sheet formulation of the water wave problem [13]. Travelling waves are computed at different values of total displacement $h = \max(y) - \min(y)$ and Bond number $\sigma = g/k^2\tau$ (here, τ is the surface tension coefficient, k is a representative wavenumber and g is the acceleration due to gravity). The branches are continuous in both parameters. We observe that the amplitude along a branch is either limited topologically, by a profile that self-intersects or by a turning point, in which case, the largest profile is a stationary (i.e. standing) wave. As our preceding proof does not require positive values of gravity, we compute perturbations of the Crapper wave with both signs of σ. We allow large departures from $\sigma = 0$, computing wave profiles with $\sigma \in (-1, 20]$, in which interval we observe continuous dependence on Bond number, including at the Wilton ripple configurations [25,45,46].

The numerical method used to compute these waves is based on the method of [13]. In this method, we find functions θ and γ that solve the equations

$$U = -c\sin(\theta) \quad \text{and} \quad U_t = 0;$$

this is the travelling wave ansatz, as developed in [13]. Here, U is the normal velocity of the fluid interface and is equal to the normal component of the Birkhoff–Rott integral (which will be introduced in the following paragraph). A Fourier-collocation method is used to discretize spatial derivatives. We seek symmetric, even profiles in terms of tangent angle θ and vortex sheet strength γ. The frame of the wave is defined so that the mean of γ and θ are zero. When the system is discretized with N spatial points, we must then solve for N Fourier modes and the wave speed c. The projection of the partial differential equation into Fourier space gives N equations, to which we append an equation fixing the amplitude to close the system. The resulting nonlinear system of algebraic equations is then solved via Broyden's method, and continuation in amplitude or gravity, similar to [47,48].

The collocation method is standard, with the possible exception of the implementation of the Birkhoff–Rott integral, $\mathbf{W} = (W_1, W_2)$, given by

$$W_1 - iW_2 = \frac{1}{4\pi i}\text{PV}\int_0^{2\pi} \gamma(\beta)\cot\left(\frac{1}{2}(z(\alpha) - z(\beta))\right)d\beta,$$

which is computed using the method used in [13,49], wherein the integral is split into singular and regular parts. The singular portion is $1/2H(\gamma/z_\alpha)$, where H is the Hilbert transform and is computed using its definition in Fourier space, $\widehat{H(f)}(k) = -i\,\text{sign}(k)\hat{f}(k)$. The remainder integral, $W_1 - iW_2 - 1/2H(\gamma/z_\alpha)$, is non-singular and is computed using the trapezoidal rule at alternating grid points. The numerical results presented here use $n = 512$ spatial points, resulting in an arclength step size of $\Delta\alpha \approx 0.01$. At this resolution, the largest computed waves, which have overturned crests and are near pinch-off, have Fourier modes that decay to 10^{-8} by wavenumber $k = 256$.

We observe that travelling waves depend continuously on Bond number. The waves are also continuous in amplitude, and we use this fact to continue in both parameters to find the largest amplitude waves. As our numerical method is based on a vortex sheet formulation, we cannot compute waves that self-intersect, like those in [36,39] (that is, for self-intersecting waves, we would be unable to compute the Birkhoff–Rott integral). We are able to compute waves very close to the first self-intersecting configuration, which we refer to as pinch-off. The Crapper wave first self-intersects when the scaled displacement $h/2\pi = (\max(y) - \min(y))/2\pi = 0.73$ [1,10]. We have computed overturned profiles with scaled displacements up to $h/2\pi = 0.723$, or 99% of the Crapper pinch-off displacement. Computed Crapper wave profiles at a sampling of amplitudes are superimposed in figure 1a.

An advantage of quasi-Newton-based methods over amplitude expansions, like Hogan [22] or Haupt & Boyd [37], is that no modification is necessary to compute travelling waves at the Wilton ripple resonant configurations. We observe Wilton ripples that are continuously embedded in the branches of travelling waves. In figure 1b, the profiles of travelling waves are presented for $\|y\|_\infty = 0.2$ at a sampling of Bond numbers $\sigma \in [-0.95, 20]$.

We have employed continuation schemes to follow continuous branches of travelling waves in both amplitude and Bond number. Beginning with the Crapper wave, we observe that waves become more localized with increased Bond number. As σ increases, profiles become more solitary than periodic, gaining oscillatory tails similar to those computed in [47,50]. These changes occur at all amplitudes, see figure 1 for the case of $\|y\|_\infty = 0.2$, however, the size of oscillations in the tail decreases with amplitude. These numerical results support the argument of Longuet-Higgins [39], that the large-amplitude Crapper wave is connected continuously to gravity–capillary solitary waves. It is natural that the waves become solitary, as increasing the Bond number has the dual interpretation of decreasing k and increasing the wavelength.

In figure 2, we report both the globally largest wave and a phase portrait of the existence of travelling waves in the gravity–displacement plane. We observe that branches of travelling waves

11

rspa.royalsocietypublishing.org   Proc. R. Soc. A **470**: 20130526
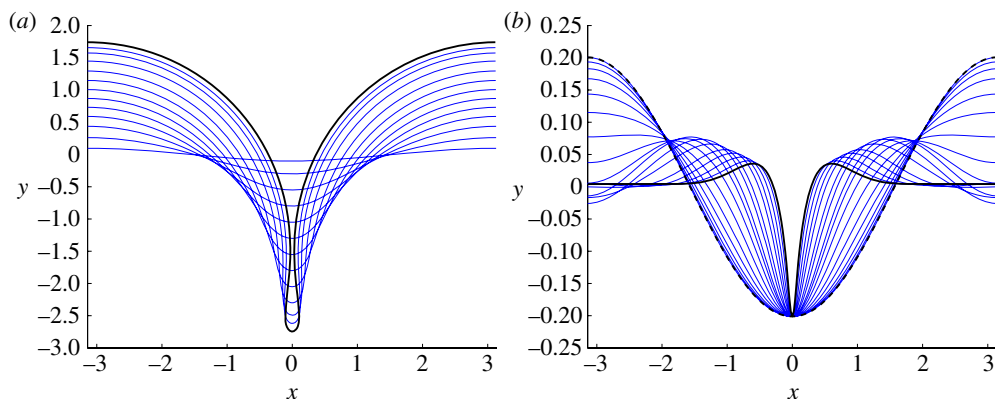
Figure 1. (a) Crapper waves with $g = 0$, at different displacements. The largest computed wave has scaled displacement $h/2\pi = 0.723$. (b) Travelling wave profiles with $\|y\|_\infty = 0.2$ for different values of the Bond number $\sigma \in [-0.95, 20]$. The wave profiles deform continuously from the sinusoidal wave with $\sigma = -0.95$, marked with a dashed curve, towards a gravity–capillary solitary wave, similar to the profile with $\sigma = 20$, marked with a thick solid line. (Online version in colour.)
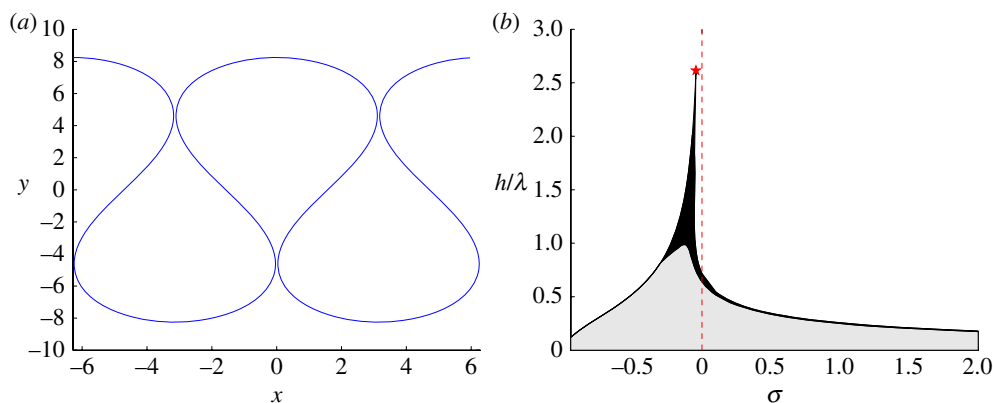
Figure 2. (a) Two periods of the profile of the largest computed water wave interface are plotted as a function of the horizontal coordinate. This wave is marked by a star in (b). This wave has $\sigma \approx -.0432$, and $h/\lambda \approx 2.62$, more than triple that of the first self-intersecting Crapper wave. (Here, $\lambda = 2\pi$ is the horizontal period.) (b) A phase portrait displays the regions of gravity–displacement space where single-valued (grey) travelling waves and multi-valued (black) travelling waves exist. The boundary with the white region is either a self-intersecting wave, to the right of the star, or a standing wave, to the left of the star. The globally largest wave is both standing and self-intersecting and is marked by the star. (Online version in colour.)

culminate in one of two ways: either in a standing wave or a self-intersecting profile. We consider self-intersecting interfaces to be the terminus of a branch of travelling waves. It is possible that branches of travelling waves continue to exist after self-intersection, however, such profiles need to be computed with an alternative method, for example, that of [36]. In figure 2b, we report a phase portrait of the space of travelling waves. In the grey region, travelling waves are single-valued functions of the x-coordinate. In the black region, the waves have overturned crests. The boundary between the black and white region is an estimate of the displacement of the largest wave. This boundary corresponds to self-intersection of the wave profile to the right of the star and a standing wave ($c = 0$) to the left of the star. The globally largest wave is marked by a star, and is both stationary and self-intersecting.

That travelling waves exist with negative Bond numbers (owing to negative gravity coefficients) is not surprising when one examines the linear situation. The speed of a linear wave is $c_p = \pm\sqrt{1 + \sigma}$. One might expect travelling waves whenever the phase speed is real—thus

12

rspa.royalsocietypublishing.org *Proc. R. Soc. A* **470**: 20130526
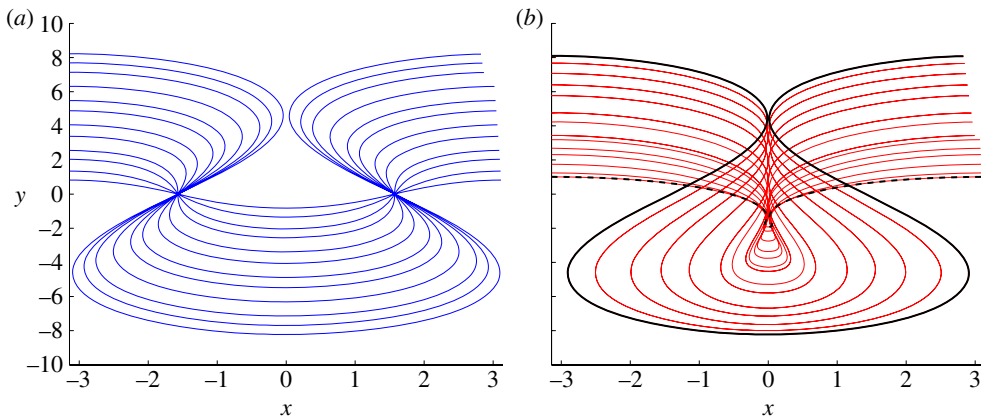
Figure 3. (*a*) The largest computed waves to the left of the star in figure 2, with $\sigma \in (-1, -0.0432)$. These profiles are all standing waves. (*b*) The largest computed waves to the right of the star in figure 2, for $\sigma \in (-0.0432, 0.2]$. In this range, the largest travelling wave profile self-intersects, entraining a bubble at its trough. Both the length and breadth of the bubble are decreasing functions of Bond number. The largest profile, marked with the thicker solid black line, is marked with the star in figure 2 and has $\sigma \approx -0.0432$. The smallest profile has $\sigma = 0.2$, and is marked by the black dashed line. (Online version in colour.)

linear theory predicts travelling waves for $\sigma > -1$. When $\sigma = -1$, the speed of the wave is zero, and we are left with stationary, standing waves. This is exactly what we observe numerically. Moreover, we observe that for the most negative Bond numbers, the branches of nonlinear travelling waves have amplitudes limited by standing waves. These standing waves form the boundary of the white region in figure 2*b*, from $\sigma = -1$ to $\sigma \approx -0.0432$ marked by the star. Profiles of these standing waves are shown in figure 3*a*. The water wave problem has a symmetry between waves moving to the left and right. Given a wave of a particular amplitude and speed, there is a corresponding wave with the same amplitude and negative speed. At stationary waves, these two branches of travelling waves intersect to form a closed loop. Whenever branches of travelling waves are thus connected, the standing wave will be the profile of limiting amplitude.

References

1. Crapper GD. 1957 An exact solution for progressive capillary waves of arbitrary amplitude. *J. Fluid Mech.* **2**, 532–540. (doi:10.1017/S0022112057000348)

13

rspa.royalsocietypublishing.org Proc. R. Soc. A 470: 20130526

2. Crapper GD. 1984 *Introduction to water waves*. Ellis Horwood Series: Mathematics and its Applications. Chichester, UK: Ellis Horwood Ltd.

3. Kinsman B. 2012 *Wind waves: their generation and propagation on the ocean surface*. New York, NY: Dover Publications.

4. Kinnersley W. 1976 Exact large amplitude capillary waves on sheets of fluid. *J. Fluid Mech.* **77**, 229–241. (doi:10.1017/S0022112076002085)

5. Tanveer S. 1996 Some analytical properties of solutions to a two-dimensional steadily translating inviscid bubble. *Proc. R. Soc. Lond. A* **452**, 1397–1410. (doi:10.1098/rspa.1996.0071)

6. Crowdy DG. 2000 A new approach to free surface Euler flows with capillarity. *Stud. Appl. Math.* **105**, 35–58. (doi:10.1111/1467-9590.00141)

7. Crowdy DG. 2000 Hele-Shaw flows and water waves. *J. Fluid Mech.* **409**, 223–242. (doi:10.1017/S0022112099007685)

8. Okamoto H. 2005 Uniqueness of Crapper's pure capillary waves of permanent shape. *J. Math. Sci. Univ. Tokyo* **12**, 67–75.

9. Okamoto H, Shōji M. 2001 The mathematical theory of permanent progressive water-waves. In *Advanced series in nonlinear dynamics*, vol. 20. River Edge, NJ: World Scientific Publishing Co. Inc.

10. Tiron R, Choi W. 2012 Linear stability of finite-amplitude capillary waves on water of infinite depth. *J. Fluid Mech.* **696**, 402–422. (doi:10.1017/jfm.2012.56)

11. Hogan SJ. 1988 The superharmonic normal mode instabilities of nonlinear deep-water capillary waves. *J. Fluid Mech.* **190**, 165–177. (doi:10.1017/S0022112088001260)

12. Chen B, Saffman PG. 1985 Three-dimensional stability and bifurcation of capillary and gravity waves on deep water. *Stud. Appl. Math.* **72**, 125–147.

13. Akers B, Ambrose DM, Wright JD. 2013 Traveling waves from the arclength parameterization: vortex sheets with surface tension. *Interf. Free Bound.* **15**, 359–380.

14. Hou TY, Lowengrub JS, Shelley MJ. 1994 Removing the stiffness from interfacial flows with surface tension. *J. Comput. Phys.* **114**, 312–338. (doi:10.1006/jcph.1994.1170)

15. Hou TY, Lowengrub JS, Shelley MJ. 1997 The long-time motion of vortex sheets with surface tension. *Phys. Fluids* **9**, 1933–1954. (doi:10.1063/1.869313)

16. Ambrose DM. 2003 Well-posedness of vortex sheets with surface tension. *SIAM J. Math. Anal.* **35**, 211–244. (doi:10.1137/S0036141002403869)

17. Baker GR, Meiron DI, Orszag SA. 1982 Generalized vortex methods for free-surface flow problems. *J. Fluid Mech.* **123**, 477–501. (doi:10.1017/S0022112082003164)

18. Saffman PG, Yuen HC. 1982 Finite-amplitude interfacial waves in the presence of a current. *J. Fluid Mech.* **123**, 459–476. (doi:10.1017/S0022112082003152)

19. Meiron DI, Saffman PG. 1983 Overhanging interfacial gravity waves of large amplitude. *J. Fluid. Mech.* **129**, 213–218. (doi:10.1017/S0022112083000737)

20. Turner REL, Vanden-Broeck J-M. 1986 The limiting configuration of interfacial gravity waves. *Phys. Fluids* **29**, 372–375. (doi:10.1063/1.865721)

21. Grimshaw RHJ, Pullin DI. 1986 Extreme interfacial waves. *Phys. Fluids* **29**, 2802–2807. (doi:10.1063/1.865477)

22. Hogan SJ. 1980 Some effects of surface tension on steep water waves. Part 2. *J. Fluid Mech.* **96**, 417–445. (doi:10.1017/S0022112080002200)

23. Stokes G. 1847 On the theory of oscillatory waves. *Trans. Camb. Phil. Soc.* **8**, 441–455.

24. Craik ADD. 2005 George Gabriel Stokes on water wave theory. *Annu. Rev. Fluid Mech.* **37**, 23–42. (doi:10.1146/annurev.fluid.37.061903.175836)

25. Wilton JR. LXXII. 1915 On ripples. *Phil. Mag.* **29**, 688–700.

26. Roberts AJ. 1983 Highly nonlinear short-crested water waves. *J. Fluid Mech.* **135**, 301–321. (doi:10.1017/S0022112083003092)

27. Schwartz LW. 1974 Computer extension and analytic continuation of Stokes' expansion for gravity waves. *J. Fluid Mech.* **62**, 553–578. (doi:10.1017/S0022112074000802)

28. Roberts AJ, Schwartz LW. 1983 The calculation of nonlinear short-crested gravity waves. *Phys. Fluids* **26**, 2388. (doi:10.1063/1.864422)

29. Roberts AJ, Peregrine DH. 1983 Notes on long-crested water waves. *J. Fluid Mech.* **135**, 323–335. (doi:10.1017/S0022112083003109)

30. Nicholls DP, Reitich F. 2006 Stable, high-order computation of traveling water waves in three dimensions. *Eur. J. Mech. B, Fluids* **25**, 406–424. (doi:10.1016/j.euromechflu.2005.11.003)

31. Akers B, Nicholls DP. 2010 Traveling waves in deep water with gravity and surface tension. *SIAM J. Appl. Math.* **70**, 2373–2389. (doi:10.1137/090771351)

32. Dias F, Kharif C. 1999 Nonlinear gravity and capillary–gravity waves. *Annu. Rev. Fluid Mech.* **31**, 301–346. (doi:10.1146/annurev.fluid.31.1.301)

33. Debiane M, Kharif C. 1996 A new limiting form for steady periodic gravity waves with surface tension on deep water. *Phys. Fluids* **8**, 2780. (doi:10.1063/1.869066)

34. Debiane M, Kharif C, Amaouche M. 2000 A new method for the calculation of steady periodic capillary–gravity waves on water of arbitrary uniform depth. *Eur. J. Mech. B, Fluids* **19**, 855–870. (doi:10.1016/S0997-7546(00)00134-5)

35. Schwartz LW, Vanden-Broeck J-M. 1979 Numerical solution of the exact equations for capillary–gravity waves. *J. Fluid Mech.* **95**, 119–139. (doi:10.1017/S0022112079001373)

36. Vanden-Broeck J-M, Keller JB. 1980 A new family of capillary waves. *J. Fluid Mech.* **98**, 161–169. (doi:10.1017/S0022112080000080)

37. Haupt SE, Boyd JP. 1988 Modeling nonlinear resonance: a modification to the Stokes' perturbation expansion. *Wave Motion* **10**, 83–98. (doi:10.1016/0165-2125(88)90008-X)

38. Akers BF, Gao W. 2012 Wilton ripples in weakly nonlinear model equations. *Commun. Math. Sci.* **10**, 1015–1024. (doi:10.4310/CMS.2012.v10.n3.a15)

39. Longuet-Higgins MS. 1988 Limiting forms for capillary–gravity waves. *J. Fluid Mech.* **194**, 351–375. (doi:10.1017/S0022112088003027)

40. Helson H. 1983 *Harmonic analysis*. Reading, MA: Addison-Wesley.

41. Levi-Civita T. 1924 Determinazione rigorosa delle onde irrotazionali periodiche in acqua profonda. *Rend. Accad. Lincei.* **33**, 141–150.

42. Hur VM. 2012 No solitary waves exist on 2D deep water. *Nonlinearity* **25**, 3301. (doi:10.1088/0951-7715/25/12/3301)

43. Toland JF. 2002 On a pseudo-differential equation for Stokes waves. *Arch. Ration. Mech. Anal.* **162**, 179–189. (doi:10.1007/s002050200195)

44. Hunter JK, Nachtergaele B. 2001 *Applied analysis*. River Edge, NJ: World Scientific Publishing Co. Inc.

45. J.-M. Vanden-Broeck. 2002 Wilton ripples generated by a moving pressure distribution. *J. Fluid Mech.* **451**, 193–201. (doi:10.1017/S0022112001006929)

46. McGoldrick LF. 1970 On Wilton's ripples: a special case of resonant interactions. *J. Fluid Mech* **42**, 193–200. (doi:10.1017/S0022112070001179)

47. Akers B, Milewski PA. 2010 Dynamics of three-dimensional gravity–capillary solitary waves in deep water. *SIAM J. Appl. Math.* **70**, 2390–2408. (doi:10.1137/090758386)

48. Vanden-Broeck J-M, Dias F. 1992 Gravity–capillary solitary waves in water of infinite depth and related free surface flows. *J. Fluid Mech.* **240**, 549–557. (doi:10.1017/S0022112092000193)

49. Ambrose DM, Wilkening J. 2010 Computation of symmetric, time-periodic solutions of the vortex sheet with surface tension. *Proc. Natl Acad. Sci. USA* **107**, 3361–3366. (doi:10.1073/pnas.0910830107)

50. Milewski PA, Vanden-Broeck J-M, Wang Z. 2010 Dynamics of steep two-dimensional gravity–capillary solitary waves. *J. Fluid Mech.* **664**, 466–477. (doi:10.1017/S0022112010004714)